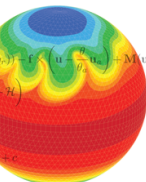


Physics coupling with the Finite-Volume Module of IFS

Christian Kühnlein, Sylvie Malardel, Piotr Smolarkiewicz, Nils Wedi

$$\begin{aligned}\frac{\partial \mathcal{G}\rho}{\partial t} + \nabla \cdot (\mathbf{v}\mathcal{G}\rho) &= 0 \\ \frac{\partial \mathcal{G}\rho \mathbf{u}}{\partial t} + \nabla \cdot (\mathbf{v}\mathcal{G}\rho \mathbf{u}) &= \mathcal{G}\rho \left(-\Theta_d \tilde{\mathbf{G}} \nabla \varphi' - \frac{\mathbf{g}}{\theta_a} (\theta' + \theta_a(\epsilon q'_v - p_v - q_r)) - \mathbf{f} \times \left(\mathbf{u} - \frac{\partial}{\partial \epsilon} \mathbf{u}_a \right) + \mathbf{M}(\mathbf{u}) + \mathbf{D} \right) \\ \frac{\partial \mathcal{G}\rho \theta'}{\partial t} + \nabla \cdot (\mathbf{v}\mathcal{G}\rho \theta') &= \mathcal{G}\rho \left(-\tilde{\mathbf{G}}^T \mathbf{u} \cdot \nabla \theta_a - \frac{L}{c_p \pi} \left(\frac{\Delta q_{vs}}{\Delta t} + E_c \right) + \mathcal{H} \right) \\ \frac{\partial \mathcal{G}\rho q_k}{\partial t} + \nabla \cdot (\mathbf{v}\mathcal{G}\rho q_k) &= \mathcal{G}\rho \mathcal{R}^{q_k} \\ \frac{\partial \mathcal{G}\rho \varphi'}{\partial t} + \nabla \cdot (\mathbf{v}\mathcal{G}\rho \varphi') &= \mathcal{G}\rho \sum_{\ell=1}^3 \left(\frac{a_\ell}{\zeta_\ell} \nabla \cdot \zeta_\ell (\hat{\mathbf{v}} - \tilde{\mathbf{G}}^T \mathbf{C} \nabla \varphi') \right) + b_\varphi + c\end{aligned}$$


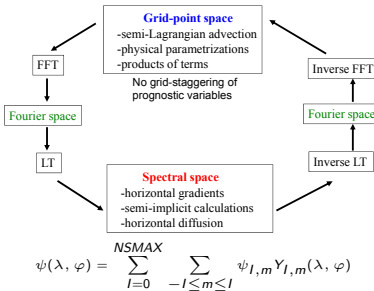


Operational configuration of the Integrated Forecasting System at ECMWF

Current operational dynamical core configuration of the Integrated Forecasting System (IFS) at the ECMWF:

- hydrostatic primitive equations (nonhydrostatic option available; see Benard et al. 2014)
- hybrid $\eta - p$ vertical coordinate (Simmons and Burridge, 1982)
- spherical harmonics representation in horizontal (Wedi et al., 2013)
- finite-element discretisation in vertical (Untch and Hortal, 2004)
- semi-implicit semi-Lagrangian (SISL) integration scheme (Temperton et al. 2001, Diamantakis 2014)
- cubic-octahedral ("TCo") grid (Wedi, 2014, Malardel et al. 2016)
- HRES: TCo1279 (O1280) with $\Delta_h \approx 9$ km and 137 vertical levels
- ENS (1+50 perturbed members): TCo639 (O640) with $\Delta_h \approx 18$ km and 91 vertical levels

Schematic of spectral-transform method in IFS

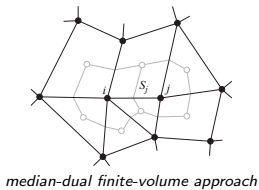


- IFS physics parametrizations for radiation, sub-grid scale turbulence and surface interaction, orographic/non-orographic drag, moist convection, clouds and stratiform precipitation, surface processes
- Fractional stepping within different parametrizations (Beljaars 1991)
- Coupling of IFS physics parametrizations to dynamical core using SLAVEPP (Semi-Lagrangian Averaging of Physical Parametrizations, Wedi 1999)



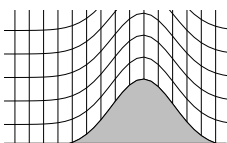
Finite-Volume Module of IFS—key formulation features

- moist-precipitating, deep-atmosphere, nonhydrostatic, fully compressible equations (Smolarkiewicz, Kühnlein, Grabowski 2017; Kühnlein et al. *in prep.*)
- flexible height-based terrain-following vertical coordinate
- hybrid of horizontally-unstructured median-dual finite-volume with vertically-structured finite-difference/finite-volume discretisation (Szmelter and Smolarkiewicz 2010; Smolarkiewicz et al. 2016)
- two-time-level semi-implicit integration scheme with 3D implicit acoustic, buoyant and rotational modes (Smolarkiewicz, Kühnlein, Wedi 2014)
- finite-volume non-oscillatory forward-in-time (NFT) MPDATA scheme (Smolarkiewicz and Szmelter 2005; Kühnlein and Smolarkiewicz 2017), directionally-split NFT advective transport (Kühnlein et al., *in prep.*)
- preconditioned generalised conjugate residual iterative solver for 3D elliptic problems arising in the semi-implicit integration schemes (Smolarkiewicz and Szmelter 2011 for a more recent review)
- octahedral reduced Gaussian grid, but the IFS-FVM formulation not restricted to this (Szmelter and Smolarkiewicz 2016)
- optional moving mesh capability (Kühnlein, Smolarkiewicz, Dörnbrack 2012)
- coupling of IFS physics parametrizations using Euler forward approach (see below)



$$\int_{\Omega} \nabla \cdot \mathbf{A} = \int_{\partial\Omega} \mathbf{A} \cdot \mathbf{n} = \frac{1}{V_i} \sum_{j=1}^{l(i)} A_j^\perp S_j$$

dual volume: V_i , face area: S_j



terrain-following coordinate

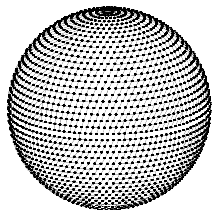


Main formulation features of IFS-ST and IFS-FVM

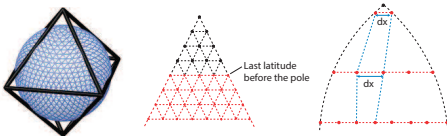
Summary of the main formulation features of IFS-FVM and IFS-ST:

Model aspect	IFS-FVM	IFS-ST	IFS-ST (NH option)
<i>Equation system</i>	fully compressible	hydrostatic primitive	fully compressible
<i>Prognostic variables</i>	$p_d, u, v, w, \theta', r_v, r_l, r_r, r_i, r_s$	$p_s, u, v, T_v, q_v, q_l, q_r, q_j, q_s$	$\pi_s, u, v, d_4, T_v, q_v, q_l, q_r, q_j, q_s$
<i>Horizontal coordinates</i>	λ, ϕ (lon-lat)	λ, ϕ (lon-lat)	λ, ϕ (lon-lat)
<i>Vertical coordinate</i>	generalized height	hybrid η -pressure	hybrid η -pressure
<i>Horizontal discretization</i>	unstructured finite-volume (FV)	spectral-transform (ST)	spectral-transform (ST)
<i>Vertical discretization</i>	structured FD/FV	structured FE	structured FD/FE
<i>Horizontal staggering</i>	co-located	co-located	co-located
<i>Vertical staggering</i>	co-located	co-located	co-located/Lorenz
<i>Horizontal grid</i>	octahedral Gaussian/arbitrary	octahedral Gaussian	octahedral Gaussian
<i>Time-stepping scheme</i>	2-TL SI	2-TL constant-coefficient SI	2-TL constant-coefficient SI
<i>Advection</i>	conservative FV Eulerian	non-conservative SL	non-conservative SL

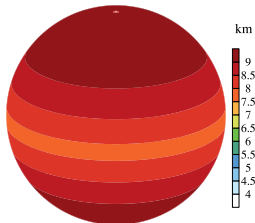
Octahedral reduced Gaussian grid



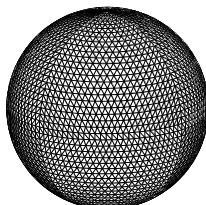
Nodes of octahedral grid O24



- suitable for spherical harmonics transforms applied in spectral IFS
- ⇒ finite-volume and spectral-transform IFS can operate on same quasi-uniform horizontal grid
- Malardel et al. ECMWF Newsletter 2016, Smolarkiewicz et al. 2016
- operational at ECMWF with HRES and ENS since March 2016
- Mesh generator and parallel data structures for IFS-FVM provided by ECMWF's Atlas framework (Deconinck et al. 2017)



Spacing of dual mesh O1280



Primary mesh about nodes of octahedral grid O24 in IFS-FVM



Governing fully compressible equations in IFS-FVM

Building on (Smolarkiewicz, Kühnlein, Grabowski 2017), flux-form fully compressible equations with moist-precipitating processes and IFS physics parametrizations (Kühnlein et al. *in prep.*):

$$\begin{aligned} \frac{\partial \mathcal{G}\rho_d}{\partial t} + \nabla \cdot (\mathbf{v}\mathcal{G}\rho_d) &= 0 , \\ \frac{\partial \mathcal{G}\rho_d \mathbf{u}}{\partial t} + \nabla \cdot (\mathbf{v}\mathcal{G}\rho_d \mathbf{u}) &= \mathcal{G}\rho_d \left[-\theta_\rho \tilde{\mathbf{G}} \nabla \varphi' + \mathbf{g}\mathcal{B} - \mathbf{f} \times \left(\mathbf{u} - \frac{\theta_\rho}{\theta_{\rho a}} \mathbf{u}_a \right) + \mathcal{M}' + \mathbf{P}^u \right] , \\ \frac{\partial \mathcal{G}\rho_d \theta'}{\partial t} + \nabla \cdot (\mathbf{v}\mathcal{G}\rho_d \theta') &= \mathcal{G}\rho_d \left[-\tilde{\mathbf{G}}^T \mathbf{u} \cdot \nabla \theta_a + P^{\theta'} \right] , \\ \frac{\partial \mathcal{G}\rho_d r_k}{\partial t} + \nabla \cdot (\mathbf{v}\mathcal{G}\rho_d r_k) &= \mathcal{G}\rho_d P^{r_k} \quad \text{where } r_k = r_v, r_l, r_r, r_i, r_s , \\ \frac{\partial \mathcal{G}\rho_d \Lambda_a}{\partial t} + \nabla \cdot (\mathbf{v}\mathcal{G}\rho_d \Lambda_a) &= \mathcal{G}\rho_d P^{\Lambda_a} , \\ \varphi' &= c_{pd} \left[\left(\frac{R_d}{\rho_0} \rho_d \theta (1 + r_v/\varepsilon) \right)^{R_d/c_{vd}} - \pi_a \right] . \end{aligned}$$

with:

$$\mathbf{v} = \tilde{\mathbf{G}}^T \mathbf{u} , \quad \theta_\rho = \frac{\theta (1 + r_v/\varepsilon)}{(1 + r_t)} , \quad \varepsilon = \frac{R_d}{R_v} , \quad \theta' = \theta - \theta_a ,$$

$$\mathcal{B} = 1 - \frac{\theta_\rho}{\theta_{\rho a}} = 1 - \frac{\vartheta}{\theta_{\rho a}} (\theta_a + \theta') , \quad \vartheta \equiv \frac{1 + r_v/\varepsilon}{1 + r_t} , \quad r_t = \sum_k r_k = r_v + r_l + r_r + r_i + r_s .$$



Integration of the fully compressible equations in IFS-FVM

Generalized transport equation:

$$\frac{\partial G\Psi}{\partial t} + \nabla \cdot (\mathbf{V}\Psi) = G \left(\mathcal{R}^\Psi + P^\Psi \right)$$

NFT template integration scheme:

$$\Psi_i^{n+1} = \mathcal{A}_i(\tilde{\Psi}, \mathbf{V}^{n+1/2}, G^n, G^{n+1}, \delta t) + b^\Psi \delta t \mathcal{R}^\Psi|_i^{n+1} \equiv \hat{\Psi}_i + b^\Psi \delta t \mathcal{R}^\Psi|_i^{n+1}$$

where

$$\tilde{\Psi} = \Psi^n + a^\Psi \delta t \mathcal{R}^\Psi|_i^n + \delta t P^\Psi|_i^n$$

and

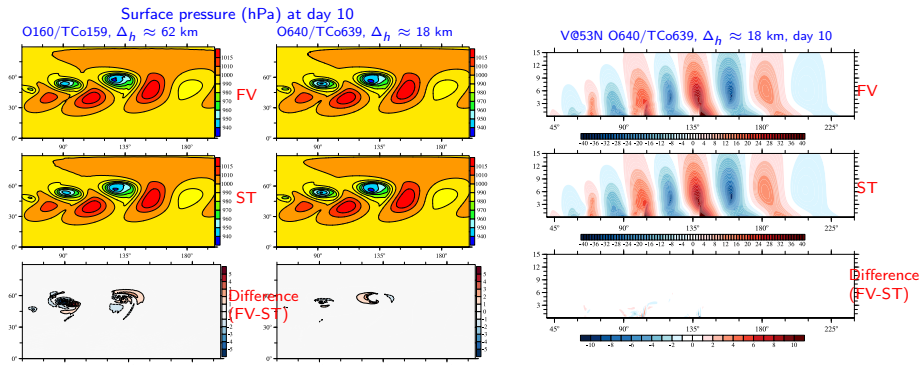
$$P^\Psi|_i^n = P^\Psi(t_{phys}, \Delta t_{phys}) \text{ where } \Delta t_{phys} = N_s \delta t \text{ and } (N_s = 1, 2, 3, \dots)$$

Prognostic variable	Ψ	\mathbf{V}	G	a^Ψ	b^Ψ
Dry density	ρ_d	$\mathbf{v}\mathcal{G}$	\mathcal{G}	-	-
Zonal physical velocity	u	$\mathbf{v}\mathcal{G}\rho_d$	$\mathcal{G}\rho_d$	0.5	0.5
Meridional physical velocity	v	$\mathbf{v}\mathcal{G}\rho_d$	$\mathcal{G}\rho_d$	0.5	0.5
Vertical physical velocity	w	$\mathbf{v}\mathcal{G}\rho_d$	$\mathcal{G}\rho_d$	0.5	0.5
Potential temperature perturbation	θ'	$\mathbf{v}\mathcal{G}\rho_d$	$\mathcal{G}\rho_d$	0.5	0.5
Water vapor mixing ratio	r_v	$\mathbf{v}\mathcal{G}\rho_d$	$\mathcal{G}\rho_d$	-	-
Liquid water mixing ratio	r_l	$\mathbf{v}\mathcal{G}\rho_d$	$\mathcal{G}\rho_d$	-	-
Rain water mixing ratio	r_r	$\mathbf{v}\mathcal{G}\rho_d$	$\mathcal{G}\rho_d$	-	-
Ice mixing ratio	r_i	$\mathbf{v}\mathcal{G}\rho_d$	$\mathcal{G}\rho_d$	-	-
Snow mixing ratio	r_s	$\mathbf{v}\mathcal{G}\rho_d$	$\mathcal{G}\rho_d$	-	-
Cloud fraction	Λ_a	$\mathbf{v}\mathcal{G}\rho_d$	$\mathcal{G}\rho_d$	-	-
Exner pressure perturbation	φ'	$\mathbf{v}\mathcal{G}\rho_d$	$\mathcal{G}\rho_d$	0	1.0



Finite-volume and spectral-transform solutions in IFS

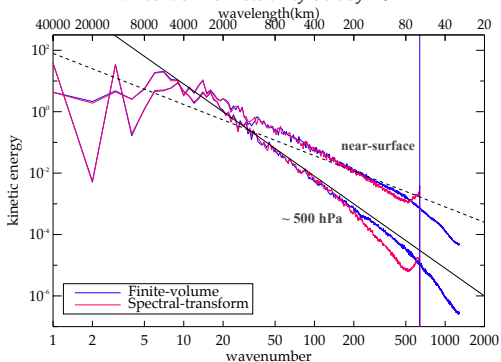
Dry baroclinic instability (Ullrich et al. 2014) using IFS-FVM and IFS-ST:



- Finite-volume solutions can achieve accuracy of established spectral-transform IFS for planetary-scale baroclinic instability

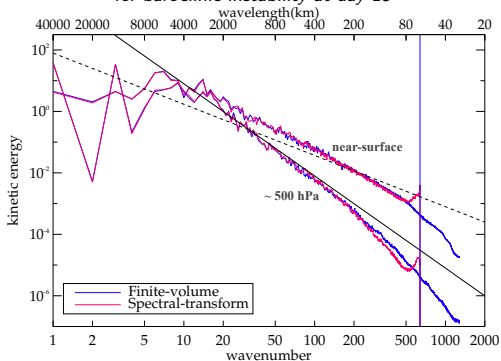


*Instantaneous kinetic energy spectra O640/TCo639 ($\Delta_h \approx 18$ km)
for baroclinic instability at day 15*



⇒ Unsplit NFT advection

*Instantaneous kinetic energy spectra O640/TCo639 ($\Delta_h \approx 18$ km)
for baroclinic instability at day 15*



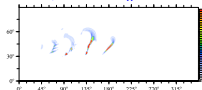
⇒ Directionally-split NFT advection

Finite-volume and spectral-transform formulations in IFS

Moist baroclinic instability using IFS-FVM and IFS-ST with parametrization for large-scale condensation and diagnostic precipitation following Reed and Jablonowski 2011:

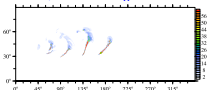
Precipitation (mm/day) at day 10

O160/TCo159, $\Delta_h \approx 62$ km



FV

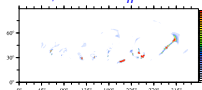
O640/TCo639, $\Delta_h \approx 18$ km



ST

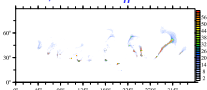
Precipitation (mm/day) at day 15

O160/TCo159, $\Delta_h \approx 62$ km



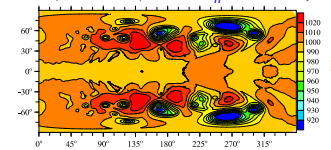
FV

O640/TCo639, $\Delta_h \approx 18$ km



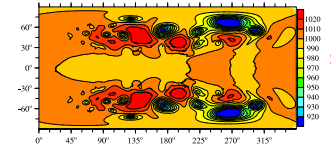
ST

Surface pressure O640/TCo639, $\Delta_h \approx 18$ km, day 15



FV

ST



- Finite-volume solutions can achieve accuracy of established spectral-transform IFS for moist flows

Finite-volume and spectral-transform formulations in IFS

Moist baroclinic instability using IFS-FVM and IFS-ST with parametrization for large-scale condensation and diagnostic precipitation following Reed and Jablonowski 2011:

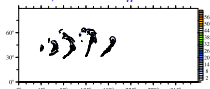
Precipitation (mm/day) at day 10

O160/TCo159, $\Delta_h \approx 62 \text{ km}$



FV

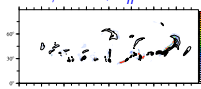
O640/TCo639, $\Delta_h \approx 18 \text{ km}$



ST

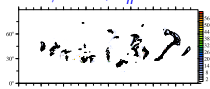
Precipitation (mm/day) at day 15

O160/TCo159, $\Delta_h \approx 62 \text{ km}$



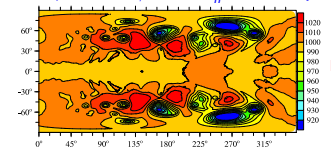
FV

O640/TCo639, $\Delta_h \approx 18 \text{ km}$



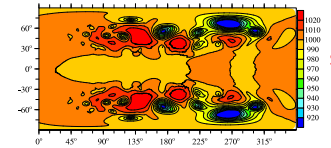
ST

Surface pressure O640/TCo639, $\Delta_h \approx 18 \text{ km}$, day 15



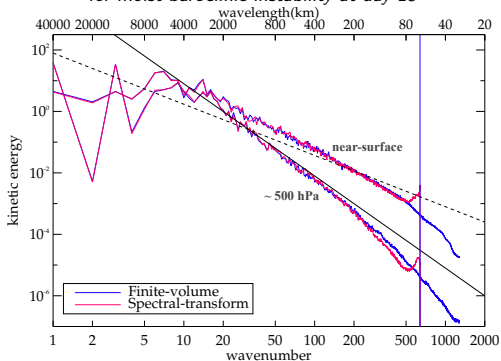
FV

ST



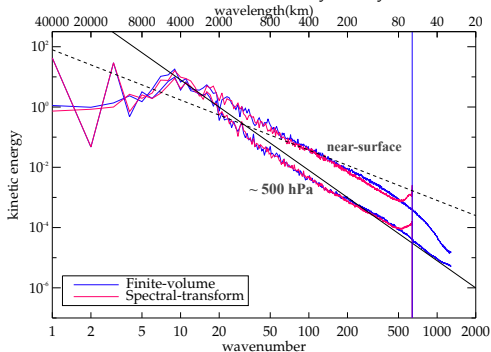
- Finite-volume solutions can achieve accuracy of established spectral-transform IFS for moist flows

*Instantaneous kinetic energy spectra O640/TCo639 ($\Delta_h \approx 18$ km)
for moist baroclinic instability at day 15*



⇒ Dry simulation with split NFT advection

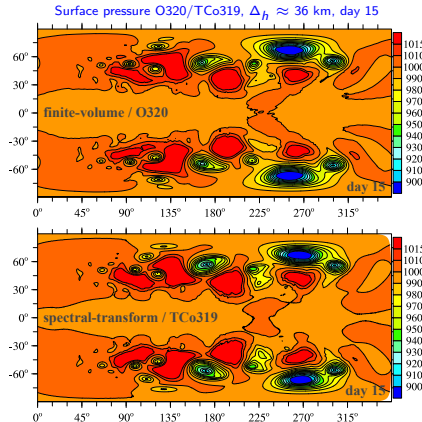
*Instantaneous kinetic energy spectra O640/TCo639 ($\Delta_h \approx 18$ km)
for moist baroclinic instability at day 15*



⇒ Moist simulation with split NFT advection

Finite-volume and spectral-transform solutions in IFS

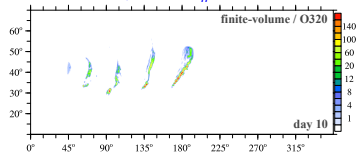
Moist-precipitating baroclinic instability using IFS-FVM and IFS-ST with IFS cloud parametrization (Forbes et al. 2010):



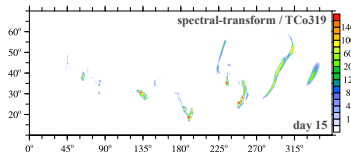
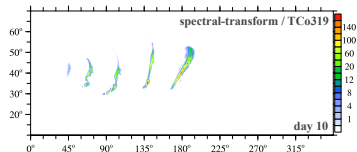
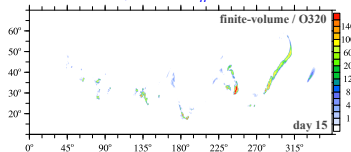
Finite-volume and spectral-transform solutions in IFS

Moist-precipitating baroclinic instability using IFS-FVM and IFS-ST with IFS cloud parametrization:

Precipitation (mm/day) at day 10
O320/TCo319, $\Delta_h \approx 36$ km



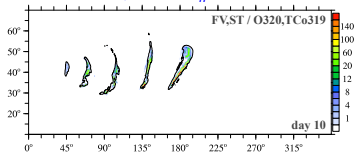
Precipitation (mm/day) at day 15
O320/TCo319, $\Delta_h \approx 36$ km



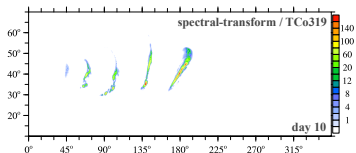
Finite-volume and spectral-transform solutions in IFS

Moist-precipitating baroclinic instability using IFS-FVM and IFS-ST with IFS cloud parametrization:

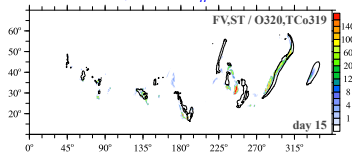
Precipitation (mm/day) at day 10
O320/TCo319, $\Delta_h \approx 36$ km



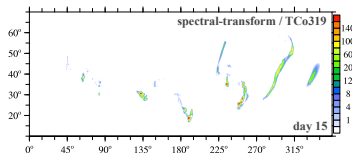
spectral-transform / TCo319



Precipitation (mm/day) at day 15
O320/TCo319, $\Delta_h \approx 36$ km

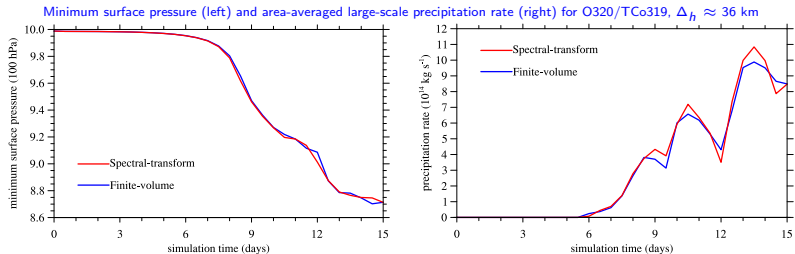


spectral-transform / TCo319



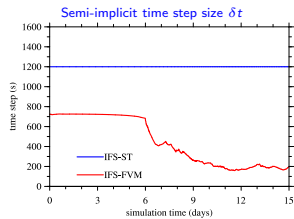
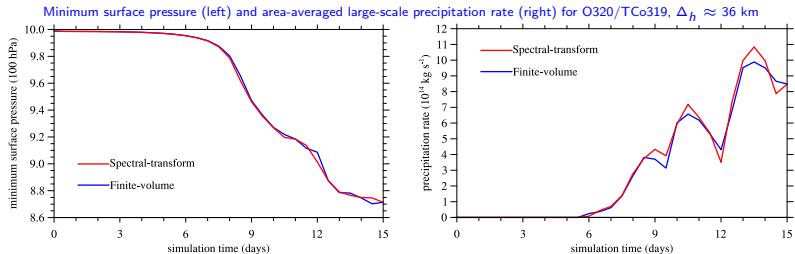
Finite-volume and spectral-transform solutions in IFS

Moist-precipitating baroclinic instability using IFS-FVM and IFS-ST with IFS cloud parametrization:



Finite-volume and spectral-transform solutions in IFS

Moist-precipitating baroclinic instability using IFS-FVM and IFS-ST with IFS cloud parametrization:



Physics-dynamics coupling in IFS-FVM: subcycling the dynamics

The IFS-FVM interface to the physics parametrizations also includes an option for subcycling of the dynamics. The template semi-implicit NFT scheme (shown on the previous slide) for one physics time step from t^N to $t^N + \Delta t_{phys} \equiv t^N + N_s \delta t$, can be written as $\ell = 1, N_s$:

$$\Psi_i(t^N + \ell \delta t) = \mathcal{A}_i(\tilde{\Psi}, \mathbf{V}(t^N + (\ell \delta t - 0.5)), G(t^N + (\ell - 1) \delta t), G(t^N + \ell \delta t), \delta t) + b^\Psi \delta t \mathcal{R}_i^\Psi(t^N + \ell \delta t) ,$$

where

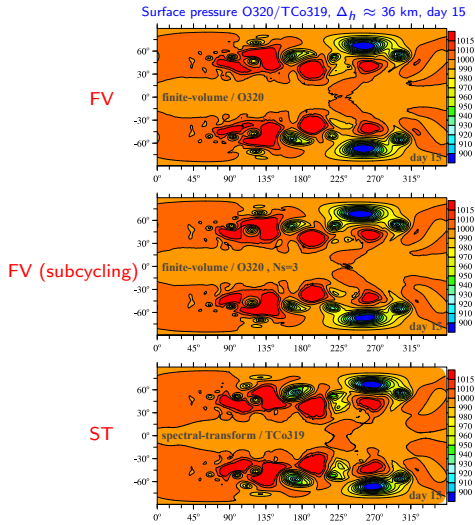
$$\tilde{\Psi} = \Psi(t^N + (\ell - 1) \delta t) + a^\Psi \delta t \mathcal{R}^\Psi(t^N + (\ell - 1) \delta t) + \delta t P^\Psi(t^N, \Delta t_{phys}) .$$

The physics tendency P^Ψ is evaluated with the physics time step Δt_{phys} and is then reused for the N_s subcycling steps with δt .



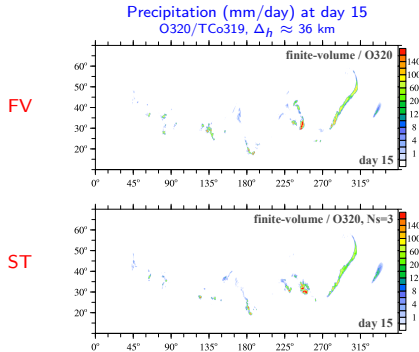
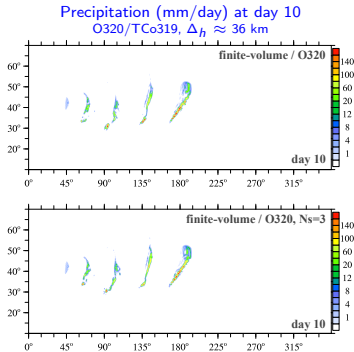
Finite-volume and spectral-transform solutions in IFS

Moist-precipitating baroclinic instability using IFS-FVM and IFS-ST with IFS cloud parametrization:



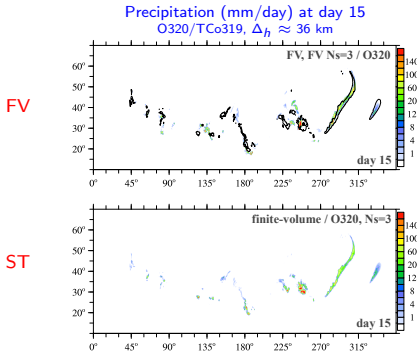
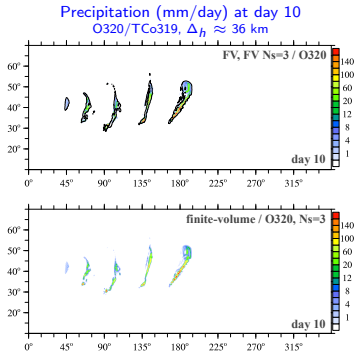
Finite-volume and spectral-transform solutions in IFS

Moist-precipitating baroclinic instability using IFS-FVM with IFS cloud parametrization (no subcycling versus subcycling of dynamics $N_s = 3$):

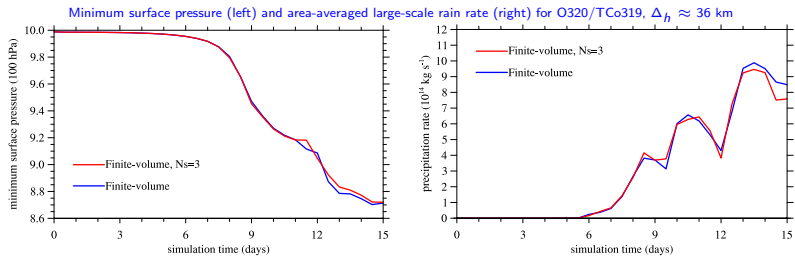


Finite-volume and spectral-transform solutions in IFS

Moist-precipitating baroclinic instability using IFS-FVM with IFS cloud parametrization (no subcycling versus subcycling of dynamics $N_s = 3$):

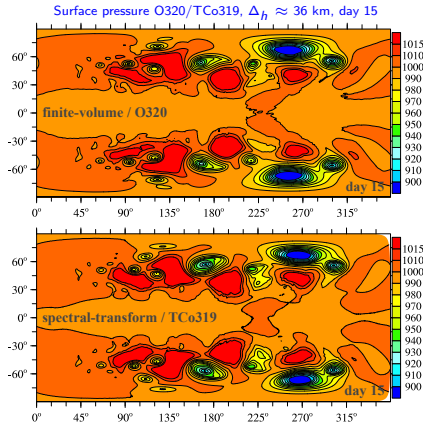


Moist-precipitating baroclinic instability using IFS-FVM with IFS cloud parametrization (no subcycling versus subcycling of dynamics $N_s = 3$):



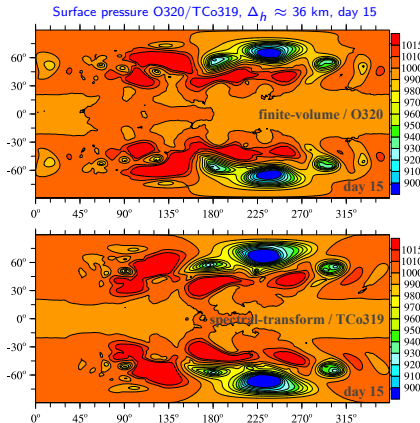
Finite-volume and spectral-transform solutions in IFS

Moist-precipitating baroclinic instability using IFS-FVM and IFS-ST with IFS cloud parametrization:



Finite-volume and spectral-transform solutions in IFS

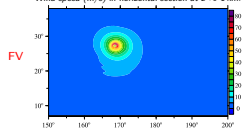
Moist-precipitating baroclinic instability using IFS-FVM and IFS-ST with IFS cloud and convection parametrization:



Finite-volume and spectral-transform solutions in IFS

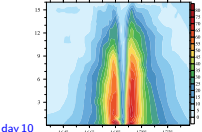
Tropical cyclone simulations with coupling to parametrisations for large-scale condensation with diagnostic rain, surface fluxes and PBL diffusion (Reed and Jablonowski 2011) on O640/L60:

Wind speed (m/s) in horizontal section at $z \approx 1\text{ km}$:



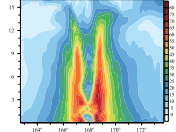
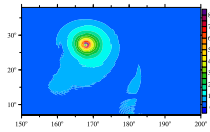
FV

Wind speed (m/s) in zonal-height section:

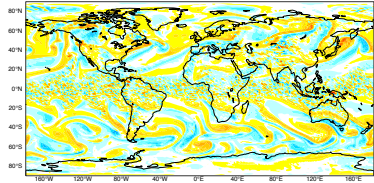


day 10

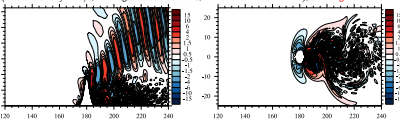
ST



Held-Suarez climate benchmark O640 (16 km) with realistic IFS orography at day 90 (relative vorticity at $z=2\text{ km}$)



stratified flow past steep orography with maximum slope $\sim 70^\circ$ on a reduced-radius planet after 2 h (vertical velocity in m/s, lon-height section at $lat=0$, lon-lat section at $z=2\text{ km}$). cf. Zängl MWR 2012



Summary and outlook

Highlights:

- IFS-FVM with generic interface to selected IFS physics parametrizations
- finite-volume versus spectral-transform semi-implicit integration schemes in geospherical framework with same grid, variable arrangement, parametrizations
- finite-volume semi-implicit integration of IFS-FVM can provide solution quality competitive to established spectral-transform IFS

Ongoing and outlook:

- coupling of IFS-FVM to full IFS physics parametrization package
- towards convection-permitting global medium-range weather forecasts
- combining methods of IFS-FVM and IFS-ST

Some relevant references

Further reading:

- Kühnlein C., P. K. Smolarkiewicz, A. Dörnbrack, Modelling atmospheric flows with adaptive moving meshes., *J. Comput. Phys.*, 2012.
- Szmelter J., P. K. Smolarkiewicz P.K, An edge-based unstructured mesh discretisation in a geospherical framework., *J. Comput. Phys.*, 2010.
- Smolarkiewicz P.K., C. Kühnlein, N. P. Wedi, A discrete framework for consistent integrations of soundproof and compressible PDEs of atmospheric dynamics., *J. Comput. Phys.*, 2014.
- Smolarkiewicz P.K., W. Deconinck, M. Hamrud, C. Kühnlein, G. Modzinski, J. Szmelter, N. P. Wedi, A finite-volume module for simulating global all-scale atmospheric flows., *J. Comput. Phys.*, 2016.
- Kühnlein C., Smolarkiewicz P.K., An unstructured-mesh finite-volume MPDATA for compressible atmospheric dynamics., *J. Comput. Phys.*, 2017.
- Smolarkiewicz P.K., C. Kühnlein, W. W. Grabowski, A finite-volume module for cloud-resolving simulations of global all-scale atmospheric flows., *J. Comput. Phys.*, 2017.
- Deconinck W., P. Bauer, M. Diamantakis, M. Hamrud, C. Kühnlein, G. Mengaldo, P. Marciel, T. Quintino, B. Raoult, P. K. Smolarkiewicz, N. P. Wedi, *Atlas: The ECMWF framework to flexible numerical weather and climate modelling.*, <https://doi.org/10.1016/j.cpc.2017.07.006>, 2017.
- Waruszewski M., C. Kühnlein, H. Pawlowska, P. K. Smolarkiewicz, MPDATA: Third-order accuracy for arbitrary flows, *in press, JCP*.
- Smolarkiewicz P.K., C. Kühnlein, N. P. Wedi, Perturbation equations for all-scale atmospheric dynamics., *submitted to J. Comput. Phys.*
- Kühnlein C., S. Malardel, Smolarkiewicz P.K., Klein R., Wedi N.P., Finite-volume and spectral-transform formulations of IFS, *in preparation for GMD*



Some notes on IFS-FVM physics parametrization interface:

- implemented by first-order coupling at t^n , with option for subcycling the entire IFS-FVM semi-implicit dynamics
- coding incorporates relevant IFS physics routines in IFS-FVM bundle (setup, modules, phys_ec, surf, phys_radi,...)
- interface is at the level of ec_phys_drv.F90 (defined as ec_phys_drv_fvm.F90)
- example TODO's way-in/out: conversions between r_k 's and q_k 's, conversions related to height- versus pressure-based vertical coordinate, compute required quantities on interfaces, geometric quantities,...
- coupling setup in vertical such that lowest full level in IFS-FVM corresponds to lowest full level in IFS-ST
- no NPROMA blocks in IFS-FVM and Fortran pointers are used to flip vertical index in interface